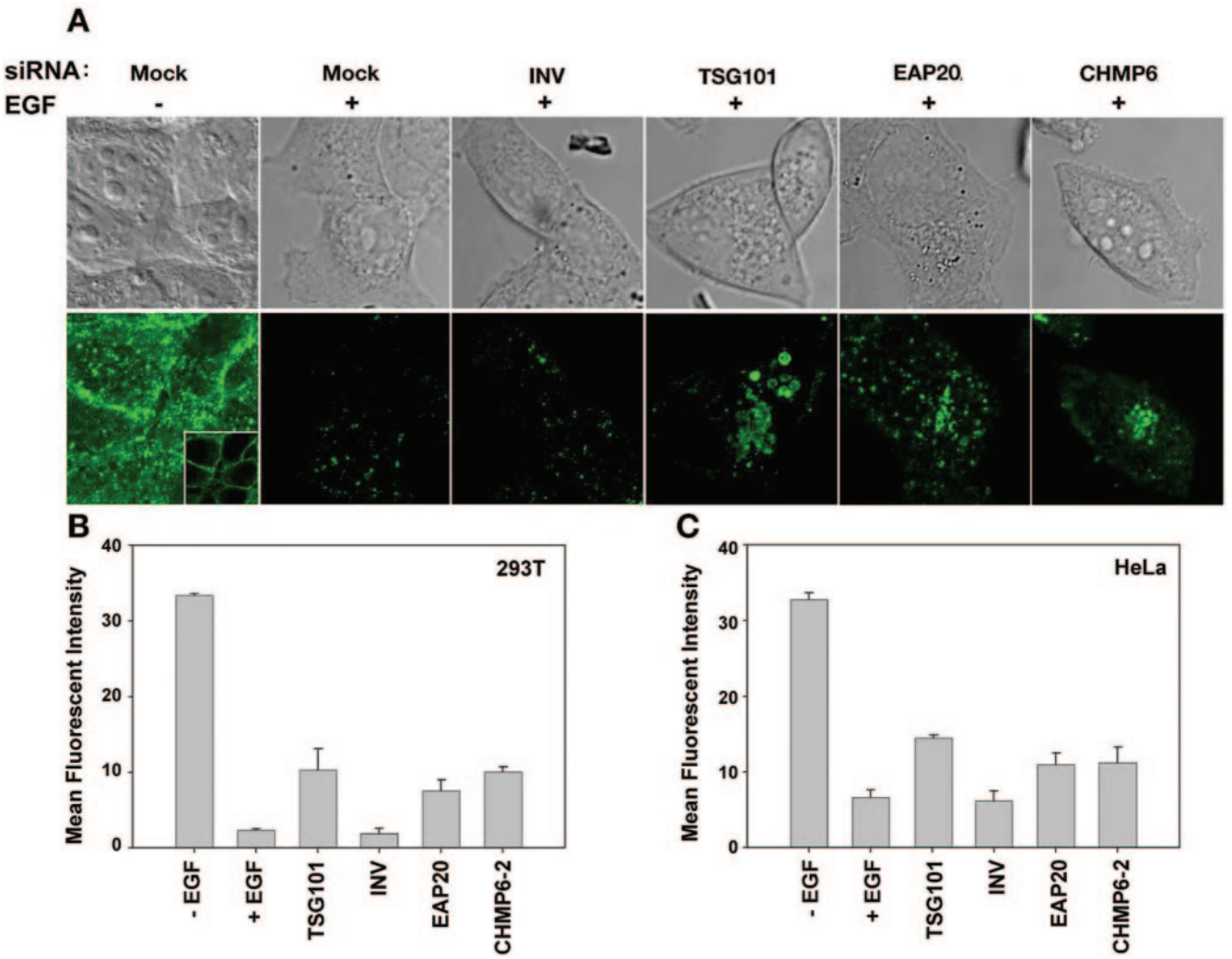

FIG. 9. EGF receptor downregulation is inhibited by depletion of TSG101, EAP20, and CHMP6. (A) 293T cells treated with siRNA were serum starved and then incubated in the presence or absence of EGF. Fixed and permeabilized cells were visualized by differential interference contrast (Nomarski) microscopy (top row) or by immunofluorescence to determine EGFR levels and localization (bottom row). Stacked whole-cell images are shown in all cases, with a central confocal slice (inset) also shown in the first image in the bottom row to demonstrate that the EGFR is located on the cell surface prior to EGF stimulation. (B) Quantification of the total levels of EGFR in 293T cells under the different conditions described for panel A. Each bar in the histogram represents the average fluorescence of individual cells as measured in three different images containing two to five cells per image. The error bars show the standard errors of the mean. The data were collected 91 h after the second siRNA transfection. (C) Quantification of total levels of EGFR in HeLa cells under the conditions described for panel A. The data were collected 92 h after the second siRNA transfection.

MVB trafficking. We note that treatment with siRNAs against TSG101 resulted in the accumulation of EGFR in larger class E compartments (17) than were seen in cells treated with siRNAs against EAP20 or CHMP6. The EGFR trafficking defects seen in the absence of ESCRT activities were similar in 293T and HeLa cells, as shown quantitatively in Fig. 9B and C. The efficiencies of protein depletion and virus release were monitored in parallel experiments that confirmed that the targeted proteins were depleted as expected and that HIV-1 release was significantly reduced by TSG101 depletion, but not by depletion of EAP20 or CHMP6 (data not shown).

Bowers et al. recently reported that siRNA depletion of EAP20 did not measurably inhibit the lysosomal degradation of MHC-I and EGF-EGFR complexes (11). This differs from our conclusion that EAP20 depletion reduced the efficiency of EGFR degradation, and we therefore investigated the issue further by testing the effects of depleting TSG101/ESCRT-I, EAP20/ESCRT-II, and CHMP6/ESCRT-III on (i) MHC-I degradation and (ii) movement of fluorescent EGF to the lysosome. In the former experiments, we found that depletion of TSG101/ESCRT-I reduced the stimulation of MHC-I receptor degradation by the Kaposi's sarcoma-associated herpesvirus ubiquitin ligase KK3 (13, 28), whereas depletion of EAP20/ESCRT-II and CHMP6/ESCRT-III did not (data not shown). These results are in excellent agreement with those of Bowers et al. (11), and we therefore conclude that efficient MHC-I downregulation requires TSG101/ESCRT-I but not EAP20/ESCRT-II or CHMP6/ESCRT-III. Thus, the ESCRT